

## Light diffusion with gain and random lasers

Diederik S. Wiersma\*

*FOM-Institute for Atomic and Molecular Physics, Kruislaan 407, 1098 SJ Amsterdam, The Netherlands  
and European Laboratory for Non-Linear Spectroscopy, Largo Enrico Fermi 2, Arcetri, 50125 Florence, Italy*

Ad Lagendijk

*FOM-Institute for Atomic and Molecular Physics, Kruislaan 407, 1098 SJ Amsterdam, The Netherlands  
and Van der Waals-Zeeman Laboratorium, Valckenierstraat 65-67, 1018 XE Amsterdam, The Netherlands*

(Received 28 February 1996)

In this paper we present calculations on light diffusion with amplification that can explain previous experiments on the spontaneous emission from such a medium. Also we discuss the experimental considerations on realizing a medium that both multiply scatters and amplifies light. In an amplifying random medium different processes can occur. We argue that one can distinguish three regimes depending on the amount of scattering, and discuss these regimes in the context of random laser action. [S1063-651X(96)05109-4]

PACS number(s): 42.25.Bs, 42.55.-f, 78.45.+h

### I. INTRODUCTION

In recent years various interesting interference effects have been recognized in light that is multiply scattered from disordered structures [1]. For instance, it was found that the interference between counterpropagating waves in disordered structures gives rise to enhanced backscattering. The phenomenon is known as coherent backscattering or weak localization [2]. Later, more interference effects were recognized such as the spatial correlations in the intensity transmitted through random media [3]. These experiments were performed on passive random media.

It is challenging to extend the field of study to active media such as laser materials. The behavior of an amplifying random medium is expected to be totally different from that of an (absorbing) passive one [4]. Since the amplification along a light path depends on the path length, the overall scattering properties depend strongly on the sample size. There is, for instance, a critical sample size, above which the intensity diverges and the system becomes unstable. In that sense, multiple light scattering with gain is similar to neutron scattering in combination with nuclear fission [5]. However, for optical gain through stimulated emission the phase of the light waves is conserved, which, in principle, allows one to study interference effects in amplifying random media. Recently coherent backscattering experiments were reported on amplifying random media [6].

An active random medium can be obtained by introducing disorder in a laser material, for instance, by grinding a laser crystal. In Sec. III we will go into the experimental considerations on realizing amplifying random media. In normal laser systems, scattering is avoided as much as possible. The laser material is placed inside an optical cavity, which results in a coherent and unidirectional output. The combination of multiple scattering with laser amplification leads to the question of whether random laser action is possible. We will discuss this issue in Sec. IV. Recently experimental studies

were published on the spontaneous emission from weakly scattering laser-dye solutions, [7] and modestly scattering powdered laser crystals [8]. In the latter study, a pulsed output was observed if the powdered laser crystal was pumped sufficiently. In Sec. II, we will present a calculation on light diffusion with optical amplification, which can explain the origin of these pulses.

#### Relevant length scales

In an amplifying random medium, light waves are both multiply scattered and amplified. The relevant length scales that describe the scattering process are the scattering mean free path  $l_s$  defined as the average distance between two scattering events, and transport mean free path  $l$  defined as the average distance a wave travels before its direction of propagation is randomized. To describe the amplification process, we have to define two more length scales: the gain length  $l_g$  and amplification length  $l_{amp}$ . The gain length is defined as the path length over which the intensity is amplified by a factor  $e^{+1}$ . The amplification length is defined as the (rms) average distance between the beginning and ending points for paths of length  $l_g$ :

$$l_{amp} = \sqrt{\frac{ll_g}{3}}. \quad (1)$$

In the limit without scattering,  $l_{amp}$  is equal to  $l_g$ . The amplification length  $l_{amp}$  and gain length  $l_g$  are the analogues of the absorption length  $l_{abs}$  and the inelastic length  $l_i$  that describe absorption.

For an amplifying random medium one can define a critical volume above which the system becomes unstable [4]. We will study samples with a slab geometry. In that case, one can define a critical thickness  $L_{cr}$  instead of a critical volume, above which the intensity diverges. The critical thickness is given by [5]

$$L_{cr} = \pi l_{amp} = \pi \sqrt{\frac{ll_g}{3}}. \quad (2)$$

Note that  $L_{cr}$  is proportional to  $l_{amp}$ .

\*Electronic address: wiersma@lens.unifi.it

## II. LIGHT PROPAGATION IN RANDOM LASER MATERIALS

For random media in which the scattering mean free path is larger than the wavelength, the propagation of light can usually be described as a diffusion process. Because almost all light scattering experiments are performed in this regime, we want to investigate some aspects of light diffusion in an amplifying medium.

We will study a slab geometry of laser material in which disorder is introduced. The laser material is assumed to be a standard four level system. We wish to study the temporal response of this disordered laser material to an incident pump and probe pulse, thereby distinguishing three frequency bands: the (green) pump light, (red) probe light, and (amplified) spontaneous emission. The energy density in these three bands is denoted by, respectively,  $W_G(\vec{r}, t)$ ,  $W_R(\vec{r}, t)$ , and  $W_A(\vec{r}, t)$ . The (narrow) spectrum of the pump and probe bands is determined by the incoming pulses, and remains unchanged. The spectrum of spontaneous emission is usually broad, however, this spectrum will narrow down upon amplification (gain narrowing). We do not consider the precise spectral properties of the output at this stage, that is, we only distinguish between the three frequency bands described above.

Assuming a diffusion process, one can describe the time- and position-dependent energy densities of pump, probe, and amplified spontaneous emission (ASE) by a diffusion equation with appropriate absorption and/or gain terms that depend on the local excitation of the system. The (also time dependent) local excitation of the system is described by the set of rate equations of the laser material. We are considering a four level laser system such as Ti:sapphire or Rhodamine 6G. This system is pumped into an excited state (2) which decays rapidly to a metastable state (1). The laser transition occurs from this metastable state to a state (0') just above the ground state, which decays rapidly to the actual ground state (0). This means that state (2) and (0') are nearly unpopulated, and that the population of state (1) can be described by one rate equation.

The total set of coupled differential equations describing our system is formed by three diffusion equations for, respectively, pump light, probe light, and amplified spontaneous emission and the rate equation for the concentration  $N_1(\vec{r}, t)$  of laser particles in state (1):

$$\begin{aligned} \frac{\partial W_G(\vec{r}, t)}{\partial t} &= D \nabla^2 W_G(\vec{r}, t) - \sigma_{\text{abs}} v [N_t - N_1(\vec{r}, t)] W_G(\vec{r}, t) \\ &+ \frac{1}{l} I_G(\vec{r}, t), \end{aligned} \quad (3)$$

$$\begin{aligned} \frac{\partial W_R(\vec{r}, t)}{\partial t} &= D \nabla^2 W_R(\vec{r}, t) + \sigma_{\text{em}} v N_1(\vec{r}, t) W_R(\vec{r}, t) \\ &+ \frac{1}{l} I_R(\vec{r}, t), \end{aligned} \quad (4)$$

$$\begin{aligned} \frac{\partial W_A(\vec{r}, t)}{\partial t} &= D \nabla^2 W_A(\vec{r}, t) + \sigma_{\text{em}} v N_1(\vec{r}, t) W_A(\vec{r}, t) \\ &+ \frac{1}{\tau_e} N_1(\vec{r}, t), \end{aligned} \quad (5)$$

$$\begin{aligned} \frac{\partial N_1(\vec{r}, t)}{\partial t} &= \sigma_{\text{abs}} v [N_t - N_1(\vec{r}, t)] W_G(\vec{r}, t) - \sigma_{\text{em}} v N_1(\vec{r}, t) \\ &\times [W_R(\vec{r}, t) + W_A(\vec{r}, t)] - \frac{1}{\tau_e} N_1(\vec{r}, t), \end{aligned} \quad (6)$$

where  $v$  is the transport velocity of the light inside the medium,  $\sigma_{\text{abs}}$  and  $\sigma_{\text{em}}$  are, respectively, the absorption and emission cross section (averaged over the relevant frequency band),  $\tau_e$  is the lifetime of the excited state (1), and  $N_t$  is the total concentration of laser particles. Here  $D$  is the diffusion constant given by

$$D = \frac{vl}{3}, \quad (7)$$

and  $I_G(\vec{r}, t)$  and  $I_R(\vec{r}, t)$  are the intensities of, respectively, the incoming pump and probe pulses. For simplicity, we use the same value of the diffusion constant for the pump and probe light, and for the ASE, although different values could easily be incorporated.

The first terms right of the equality sign in Eqs. (3)–(5) represent regular diffusion. The second terms represent respectively absorption of diffuse pump light, stimulated emission of diffuse probe light, and stimulated emission of ASE. The third terms in Eqs. (3) and (4) represent the scattering of, respectively, the coherent pump and probe pulse [9]. The third term in Eq. (5) represents spontaneous emission.

The probe pulse is incident on the front sample interface. The pump pulse is either incident on both the front and rear interface or on the front interface only. In the latter case we have

$$I_G(\vec{r}, t) = I_{G0} \sqrt{\frac{b}{\pi}} \exp[-\kappa_e z] \exp\left[-b \frac{(t - t_G - z/c)^2}{\tau_G^2}\right], \quad (8)$$

and

$$I_R(\vec{r}, t) = I_{R0} \sqrt{\frac{b}{\pi}} \exp[-\kappa_e z] \exp\left[-b \frac{(t - t_R - z/c)^2}{\tau_R^2}\right], \quad (9)$$

where  $b = 4 \ln(2)$ ,  $\kappa_e$  is the extinction coefficient, and  $c = c_0/n$ , with  $n$  the effective refractive index of the medium. Here  $I_{G0}$  and  $I_{R0}$  are the average intensities of, respectively, the pump and probe pulse,  $\tau_G$  and  $\tau_R$  are the pulse lengths full width at half maximum, and  $t_G$  and  $t_R$  denote the points in time at which the maximum of, respectively, the pump and probe pulse is incident on the sample surface. If the pump pulse is incident on both sample interfaces we modify Eq. (8) to

$$I_G(\vec{r}, t) = I_{G0} \sqrt{\frac{b \exp[-\kappa_e z] + \exp[-\kappa_e(L-z)]}{\pi}} \times \exp\left[-b \frac{(t-t_G - z/c)^2}{\tau_G^2}\right], \quad (10)$$

with  $L$  the thickness of the slab.

For a slab geometry we have the following boundary condition:

$$W_G(\vec{r}, t) = W_R(\vec{r}, t) = W_A(\vec{r}, t) = 0, \quad (11)$$

for

$$z = -z_0 \text{ and } z = L + z_0, \quad (12)$$

where  $z_0 \approx 0.71l$  is called the extrapolation length [10].

Because our system is a slab in the  $xy$  plane illuminated by plane waves in the  $z$  direction, we can omit the  $x$  and  $y$  dependence of the energy densities. This means we can retain only the partial derivative to  $z$  in the gradients in Eqs. (3)–(5).

The resulting set of coupled partial differential equations can be solved numerically using a standard (forward Euler) discretization for the time derivative:

$$\frac{\partial f(z, t)}{\partial t} := \frac{f(z, t + \Delta t) - f(z, t)}{\Delta t} \quad (13)$$

and for the second order space derivative the straightforward discretization:

$$\frac{\partial^2 f(z, t)}{\partial z^2} := \frac{f(z + \Delta z, t) - 2f(z, t) + f(z - \Delta z, t)}{\Delta z^2}. \quad (14)$$

This discretization method has the advantage that it is simple and explicit, that is, the discretization of the space derivative depends only on  $f(z, t)$  and not on  $f(z, t + \Delta t)$ . The disadvantage is that for small  $\Delta z$ , the time steps  $\Delta t$  have to be taken very small in order to satisfy the stability criterion [11]:

$$\Delta t \leq \frac{\Delta z^2}{2D}. \quad (15)$$

The physical interpretation of this criterion is that, apart from a numerical factor, the time steps have to be smaller than the diffusion time across a distance  $\Delta z$ .

### A. Results

We have solved the above set of partial differential equations numerically for various practical values of  $\sigma_{\text{abs}}$ ,  $\sigma_{\text{em}}$ , and  $\tau_e$  at different pump intensities and values of  $l$ . This provides us with all information on the spatial and temporal distribution of the three energy densities (pump light, probe light, and amplified spontaneous emission) and of the gain coefficient inside the sample. The gain coefficient is given by  $\kappa_g \equiv 1/l_g = \sigma_{\text{em}} N_1(\vec{r}, t)$ . Also we can calculate the outgoing flux at either the front or rear interface of the slab, which is determined by the gradient of the energy density at the sample interface.

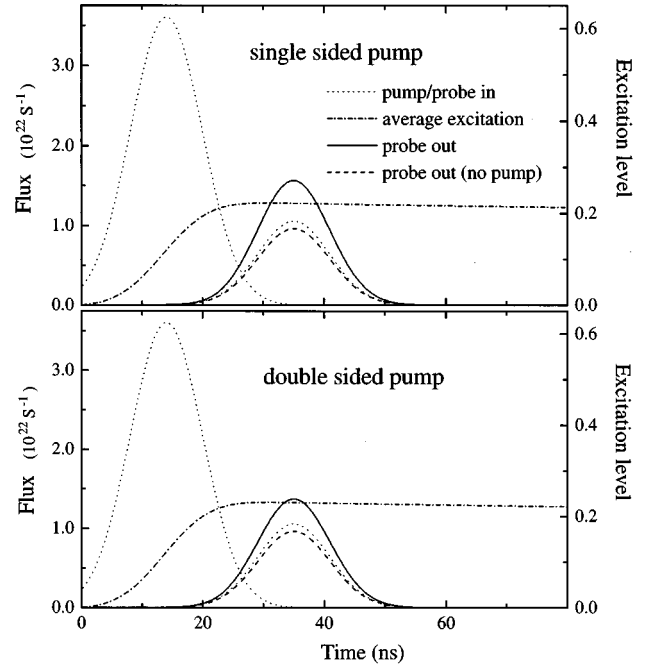


FIG. 1. Outgoing probe flux in backscattering for single sided and two sided pumping (solid line), for a powdered Ti:sapphire sample. Sample parameters: thickness 0.8 mm, diameter 4 mm, and  $l = 40 \mu\text{m}$ . Material parameters: doping level 0.15 wt %  $\text{Ti}_2\text{O}_3$  (which, at a volume fraction of 33% Ti:sapphire particles, corresponds to  $N_t = 1.6 \times 10^{25} \text{ m}^{-3}$ )  $\sigma_{\text{abs}} = 3.0 \times 10^{-24} \text{ m}^2$ ,  $\sigma_{\text{em}} = 3.0 \times 10^{-23} \text{ m}^2$ ,  $\tau_e = 3.2 \times 10^{-6} \text{ s}$ , effective refractive index  $n = 1.35$ , and  $v = c = c_0/1.35$ . In the upper graph, the sample is pumped from one side (front interface) with 14-ns pulses at 532 nm, with pulse energy 200 mJ. In the lower graph, the same pulse energy is distributed over both sample interfaces. The dashed line is the outgoing probe flux in the case where the pump is absent. The dotted line is the incoming probe and pump flux, of which the latter is scaled by a factor of  $10^3$ . The dash-dotted line denotes the average excitation level in the sample.

In Fig. 1 we have plotted the outgoing probe flux in backscattering for a powdered Ti:sapphire sample of 0.8 mm thickness and with a transport mean free path  $l = 40 \mu\text{m}$ , for two pumping geometries. In the upper graph, the sample is pumped from one side (front interface) with 14 ns pulses at 532 nm, with pulse energy 200 mJ. These sample parameters and pump energy are experimentally realistic values. In the discretization,  $\Delta z$  is taken to be  $l/2$  and  $z_0$  is taken equal to be  $l$ . The discretization error is estimated and found to be negligibly small, by repeating the calculation with a smaller  $\Delta z$ . In the lower graph, the same total pump energy is incident on the sample, but now equally distributed over front and rear sample interface. The dotted lines denote the incoming pump and probe fluxes, and the dashed line denotes the outgoing probe flux in case no pump is present. The latter is slightly smaller than the incoming probe flux due to the finite sample thickness, which allows some probe flux to disappear through the rear sample interface. The ratio of the amplified outgoing probe to the outgoing probe in the case where no pump is present gives the average overall gain in backscattering. Here the overall gain is 1.63 for single sided and 1.42 for double sided pumping.

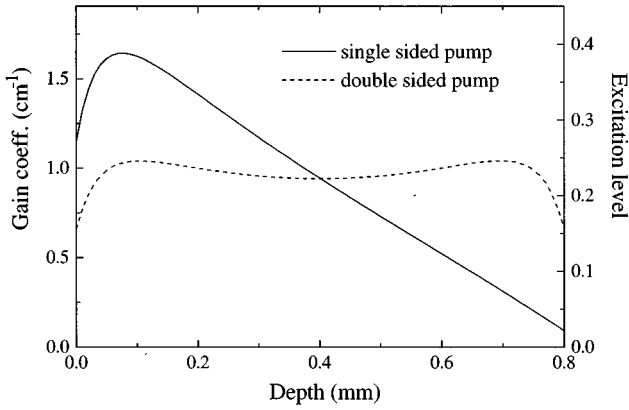


FIG. 2. Spatial profile of the excitation level just after the pump pulse, for single sided and two sided pumping, for the same sample and pump geometry as in Fig. 1. The excitation level for two sided pumping is nearly homogeneous, and its average is slightly larger than the average excitation level for single sided pumping.

The advantage of two sided pumping is that the resulting gain in the sample is nearly homogeneous. In Fig. 2, we have plotted the spatial profile of the gain coefficient just after the pump pulse for single and double sided pumping. The pump energy and the sample parameters are the same as in Fig. 1. We see that the gain coefficient drops almost linearly with increasing  $z$  for the single sided case, whereas the gain coefficient becomes almost homogeneous if we pump from two sides. Also the average gain coefficient is somewhat higher for two sided pumping. Despite this fact, the average overall gain is smaller for two sided pumping, as we saw in Fig. 1. In trying to obtain a large overall gain in backscattering, the excitation of the sample at small depth is more important than the excitation of the deeper lying parts of the sample, because the backscattered light spends on average more time in the first half of the sample.

The dash-dotted line in Fig. 1 represents the average excitation level in the sample, defined as  $N_1(\vec{r}, t)/N_1$ . After the pump pulse the excitation level decays approximately with the lifetime of the excited state ( $\tau_e = 3.2 \mu\text{s}$ ), which is much larger than the time span of the plot. At this pump intensity, the critical thickness  $L_{\text{cr}}$  remains larger than the actual sample thickness  $L$ .

If we increase the pump intensity and vary the sample thickness, we can reach the critical regime in which  $L_{\text{cr}}$  becomes smaller than  $L$  and the system becomes unstable [12]. In Fig. 3, we have plotted the temporal profile of the amplified spontaneous emission flux from a powdered Ti:sapphire sample in backscattering during and just after the pump pulse, for various pump intensities and sample thicknesses. Also plotted is the pump flux through the sample interface (dotted) and the temporal profile of the average excitation level (dashed). No probe pulse is incident in this case. Going from left to right, the sample thickness increases, and going from bottom to top, the pump flux doubles in every graph. We see that at sufficiently large pump fluxes and (or) large enough sample thicknesses, the outgoing ASE flux is pulsed.

### B. Interpretation

The pulsed behavior of the output observed in Fig. 3 originates from the combination of a diffusion process with a

time-dependent gain [4]. The relevant length scale to describe the amplification in the system is the amplification length  $l_{\text{amp}}$  as introduced before. The interpretation of the origin of this pulsed output is the following process.

(1) In the beginning of the pump pulse, the average amplification length in the medium decreases slowly due to an increasing excitation level. The time scale on which this buildup takes place is determined by the pump intensity.

(2) When  $l_{\text{amp}}$  crosses a critical value (that is, when the critical thickness given by  $L_{\text{cr}} = \pi l_{\text{amp}}$ , becomes smaller than the sample thickness), the gain in the sample becomes larger than the loss through the boundaries and the system becomes unstable. This leads to a large increase of the ASE energy density. The characteristic time scale corresponding to this buildup of ASE is  $l_g/v$ , where  $l_g$  is the gain length in the medium and  $v$  is the (transport) velocity of the light.

(3) The large ASE energy density will deexcite the system again, which leads to an increase of  $l_{\text{amp}}$ . This deexcitation continues as long as the large ASE energy density is present. The characteristic time scale on which the ASE energy density diffuses out of the medium through the front or rear interface is given by  $L^2/D$ .

An equilibrium situation would be reached when gain equals loss, i.e., when  $\pi l_{\text{amp}} = L$ . In step (2), an overshoot of the excitation takes place because the deexcitation mechanism (stimulated emission of ASE) needs a nonzero time to set in. On the other hand, once the ASE has built up considerably, the ASE energy density can disappear only slowly due to the presence of multiple scattering, which leads again to an undershoot below the equilibrium.

This process leads to (transient) oscillations in the outgoing ASE flux. Damping of these oscillations occurs, e.g., due to the fact that the increase of  $l_{\text{amp}}$  in step (3) is opposed by reexcitation due to the presence of pump light. The system reaches therefore after a few oscillations the equilibrium situation  $\pi l_{\text{amp}} = L$ .

In Fig. 3, the pump flux and the sample thickness are varied. We see that for larger pump fluxes (going from bottom to top in the graph), the oscillations start earlier and are more rapid, which is due to a more rapid decrease of  $l_{\text{amp}}$ . We also see that at larger pump fluxes the equilibrium state is reached earlier, which is due to a larger damping of the oscillations. At extremely large pump fluxes, no pulsed output is observed because the oscillations become overdamped.

Upon increasing the sample thickness  $L$  (going from left to right in the graph), the oscillations also start earlier because the situation  $\pi l_{\text{amp}} < L$  is reached at larger values of  $l_{\text{amp}}$ . The value of  $l_g$  is related to  $l_{\text{amp}}$  via  $l_{\text{amp}} = \sqrt{l_g/3}$ . Furthermore, the gain length  $l_g$  is inversely proportional to the excitation level, so the obtained excitation level is in principle [13] inversely proportional to the square of the sample thickness.

Because the characteristic time scale for the buildup of ASE is  $l_g/v$ , and the time scale for the diffusion out of the sample is  $L^2/D$ , oscillations become slower at larger sample thickness. This again leads to the fact that the equilibrium state is reached earlier at larger sample thickness.

In Fig. 4, the same graph is plotted as in Fig. 3 but now for a transport mean free path  $l$  half as long. Because  $l_{\text{amp}}$  is proportional to the square root of  $l$ , a decrease of  $l$  leads to an earlier onset of the oscillations. This again leads to larger

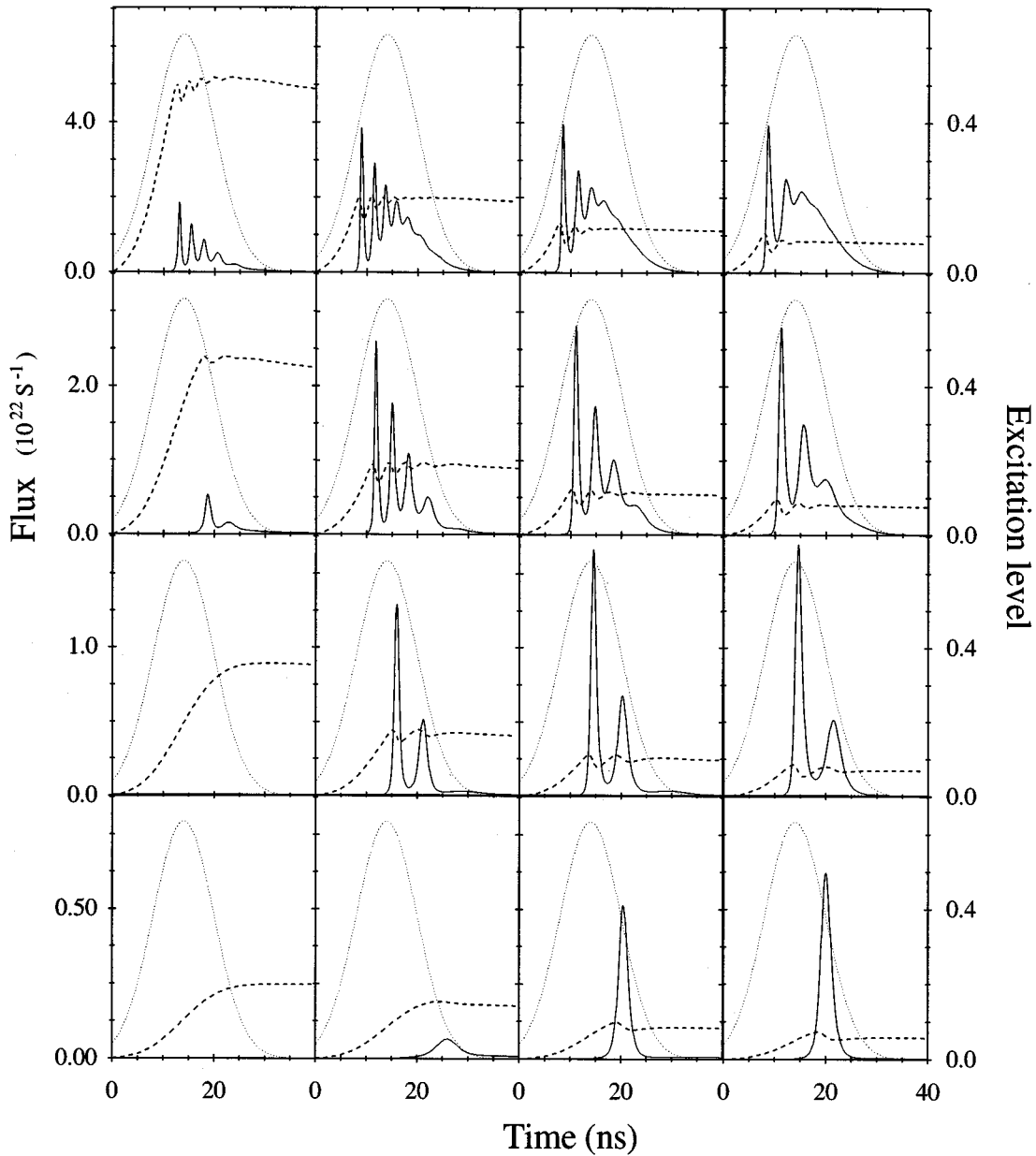


FIG. 3. Temporal profiles of the amplified spontaneous emission flux in backscattering from a powdered Ti:sapphire sample (doping level 0.15 wt %  $\text{Ti}_2\text{O}_3$ ), transport mean free path  $l = 100 \mu\text{m}$ , for different sample thicknesses and pump intensities. The pulse duration of the pump pulse is 14 ns. Also plotted is the temporal profile of the excitation level (dashed) and the pump flux (scaled by a factor  $4 \times 10^3$ ) (dotted). Sample diameter 4 mm. Going from left to right, the thickness of the sample increases in each graph with 1 mm, starting from 1 mm, and going from bottom to top, the average pump flux doubles in every graph, starting from  $3.35 \times 10^{25}$  photons/sec, which corresponds to 175 mJ at 532 nm in 14 ns.

values of  $l_g$  and correspondingly smaller values of the obtained excitation level. Due to a larger  $l_g$  and a smaller diffusion constant ( $D = vl/3$ ), the oscillations are slower and the equilibrium state is reached earlier.

The above results can explain recent observations by Gouedard *et al.*, who studied the emission from pumped hydrated neodymium powders [8]. There it was found that at large enough pump powers the output of the powder during a 6-ns pump pulse shows a pulsed behavior. These observations are consistent with the pulsed output that we have found above.

### C. Laser spiking

Most regular laser systems, when switched on, also show transient oscillations in the output, a phenomenon that is known as laser spiking [14]. The process that leads in regular lasers to spiking is similar to the process described above. In regular lasers, the photon number in the cavity also needs a nonzero time to build up after the population inversion has been pumped above its threshold value for lasing. This leads to an overshoot of the population inversion above its steady state value, followed by a spike in the output and again an undershoot of the population inversion. This process can re-

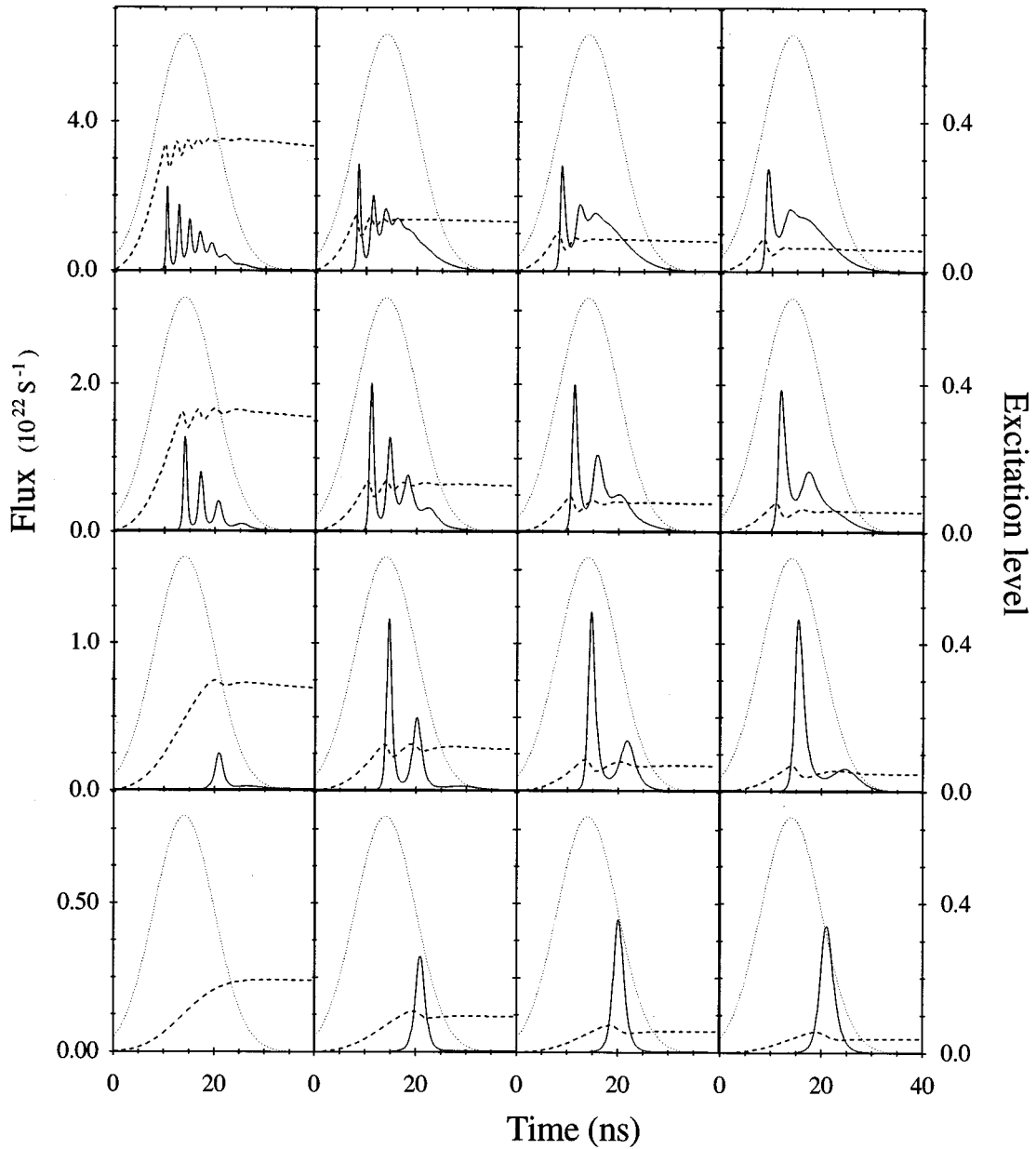


FIG. 4. Same as in Fig. 3, but for a transport mean free path half as long:  $l = 50 \mu\text{m}$ .

peat itself many times, however, most lasers are designed in such a way that these spikes die out after a few oscillations.

This similarity between regular lasers and light diffusion with gain is also apparent if we compare Eqs. (5) and (6) with the rate equations of, respectively, the photon number and population inversion of a normal laser. In both cases we have a set of coupled differential equations that are first order in time and that have similar gain and loss terms. The first and second terms of Eqs. (5) and (6) compare to, respectively, a cavity loss term and a cavity gain term. The third term of Eqs. (5) and (6) is the spontaneous emission term, which for a regular laser is only present in the rate equation of the population inversion and is missing in the rate equation of the cavity photon number.

Both sets of rate equations give rise to transient oscillations and we can compare the frequency of our oscillations with the frequency of spiking in regular lasers. The fre-

quency  $\omega_{\text{sp}}$  of spiking in normal lasers is approximately given by [14]

$$\omega_{\text{sp}} = \sqrt{R_p K - \gamma_2 \gamma_c}, \quad (16)$$

in which  $R_p$  is the pumping rate, and  $K$  is the coupling constant between the photon number and the population inversion, which is equal to  $\sigma_{\text{em}} v$ . Here  $\gamma_2$  is the decay rate of the excited state (so  $\gamma_2 = 1/\tau_e$ ) and  $\gamma_c$  is the loss rate of the cavity, which in our case is given by the first term in Eq. (5) and depends thereby on both space and time. However, we can approximate the cavity loss rate by the reciprocal of the average time the light needs to diffuse out of the sample, that is  $\pi^2 D/L^2$ . The equivalent of the pumping rate is the first term of Eq. (6), which in our case depends also on both space and time. However, the average pumping rate during the pump pulse and over the whole sample can be calculated

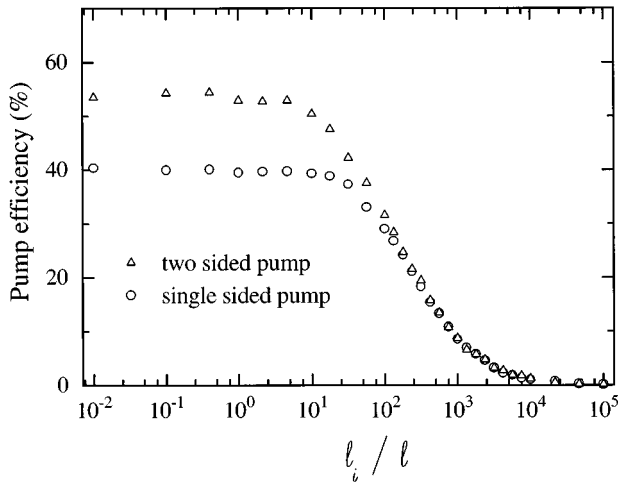


FIG. 5. Pump efficiency vs  $l_i/l$  for a single and two sided pump geometry, calculated in a Monte Carlo simulation on light diffusion in a four level laser material with disorder. The medium had a slab geometry with optical thickness 20. During the diffusion through the medium, the light was given an absorption chance at every scattering event that depended on the local excitation level of the medium [15]. The number of incident photons was chosen equal to the amount of excitable particles in the slab.

from the average pump energy that is absorbed. For instance for the parameters of Fig. 3, at sample thickness  $L=2$  mm and pump flux  $1.34 \times 10^{26} \text{ s}^{-1}$  (second row, second column), the average pumping rate is  $7.5 \times 10^{32} \text{ s}^{-1} \text{ m}^{-3}$ . This leads via Eq. (16) to  $\omega_{\text{sp}} = 2.2 \times 10^9$  or an oscillation period of 2.8 ns, which is in surprisingly good agreement with the observed oscillation period, that ranges from 3.3 to 3.7 ns.

### III. REALIZING DISORDERED MEDIA WITH GAIN

Optical amplification can be obtained in practice through stimulated emission in a laser material. To introduce scattering in such a material, one can grind a laser crystal such as ruby or Ti:sapphire. Another option is to use latex microparticles combined with laser dye, either by suspending the particles in a dye solution or by doping the particles with the dye.

To obtain amplification, the laser material must be excited, which can, for instance, be done optically. However, in a disordered medium, one encounters several problems that do not occur in conventional laser systems. In a conventional laser system, the pump light is simply absorbed by the laser material, which is thereby brought into the desired excited state. If disorder is introduced in such a laser material, the pump light will also be multiply scattered. If the scattering is much stronger than the absorption (which is generally the case for the media of interest), most of the pump light is scattered out of the system without being absorbed.

In Fig. 5 we have plotted the pump efficiency (that is, the ratio between the absorbed pump light and the total incident pump light) versus  $l_i/l$  for a slab with an optical thickness of 20. Here  $l_i$  is the inelastic mean free path if the system is in the ground state and  $l$  the transport mean free path. This pump efficiency was determined in a Monte Carlo simulation on the diffusion of pump light through a disordered laser

TABLE I. Pump efficiency for some laser materials with disorder in a single sided pump geometry. The transport mean free path is chosen:  $l = 20 \mu\text{m}$ . The inelastic mean free path  $l_i$  was calculated from the maximum absorption cross section assuming a volume fraction of, respectively, 30% powdered laser crystal or 10% latex spheres with R6G. Also listed is the required pump energy to fully excite a slab of thickness 0.4 mm and diameter 4.0 mm, taking into account the pump efficiency [16].

Material	$l_i$ (m)	$l_i/l$	Pump eff.	Pulse energy (mJ)
Latex spheres with R6G	$5.0 \times 10^{-5}$	2.5	40 %	6.0
Ti:Al <sub>2</sub> O <sub>3</sub> (0.15%)	$2.3 \times 10^{-2}$	$1.17 \times 10^3$	7.7%	351
Cr:Al <sub>2</sub> O <sub>3</sub> (0.05%)	$2.5 \times 10^{-2}$	$1.23 \times 10^3$	7.4%	122
Cr:Al <sub>2</sub> O <sub>3</sub> (2.1%)	$5.9 \times 10^{-4}$	$2.92 \times 10^1$	38%	992
Nd:YAG (1.1%)	$2.0 \times 10^{-3}$	$1.0 \times 10^2$	29%	269
Nd:glass (5.0%)	$0.9 \times 10^{-3}$	$4.5 \times 10^1$	35%	771

material (assuming a standard four level system), where the light was given an absorption chance at every scattering event that depended on the local excitation level of the medium [15].

In Table I, we have listed the value of  $l_i/l$  for a few disordered laser materials with a transport mean free path of  $l=20 \mu\text{m}$ . We see that the resulting pump efficiency can be lower than 10%. In Table I, we have also listed the pump pulse energy required for a complete excitation of a sample of optical thickness 20 and optical diameter 200. The listed pulse energies take into account the pump efficiency for a simple single sided pumping geometry.

The intensities required to excite a laser material are high, which is a complicating factor in the experiments. With a continuous wave (cw) laser, they can be obtained only if the light is focused to a diameter of a few tens of micrometers, and the resulting excited volume will therefore be very small. If we wish to excite a larger volume, we are forced to use pulsed pump light. This means that our disordered laser material will not amplify continuously, but only during some limited time window (ranging from 10 ns to several ms), at a certain repetition rate. At low pumping intensities, this window will be determined by the excited state lifetime  $\tau_e$ . At high pump intensities amplified spontaneous emission will deexcite the system thereby largely narrowing this time window.

The excited state lifetime of ruby is very large (3.0 ms). Unfortunately, this material is a three level system and therefore the absorption at the emission wavelength is large. Laser dye such as Rhodamine 6G has the advantage of a very large absorption and emission cross section ( $\sim 10^{20} \text{ m}^2$ ). However, experiments on dye using a probe pulse will have to be performed with picosecond time resolution due to the very short lifetime of the excited state ( $\sim 10^{-9} \text{ s}$ ). A good choice of laser material is Ti:sapphire because it has a reasonably large emission cross section ( $3.0 \times 10^{-23} \text{ m}^2$ ) and excited state lifetime (3.2  $\mu\text{s}$ ), and its emission wavelengths are in the visible regime.

We have performed experiments both with ruby and Ti:sapphire. The maximum pulse energy incident on the

TABLE II. Results of transmission and backscattering measurements on the overall gain from powdered ruby (2.1 wt %  $\text{Cr}_2\text{O}_3$ ) and powdered Ti:sapphire (0.15 wt %  $\text{Ti}_2\text{O}_3$ ). Pump wavelength 532 nm, pulse duration 14 ns. The ruby-air samples get burnt already at modest pump intensities. The ruby-glycerol samples show air bubbles at high intensities. With the Ti:sapphire, a large gain is obtained without damage to the sample. Only at the highest pump intensities, a slight structural change is visible for the Ti:sapphire-air sample. The gain lengths for the backscattering data are calculated using diffusion theory[6].

Transmission data						
Material	in	$L$ ( $\mu\text{m}$ )	$l$ ( $\mu\text{m}$ )	Pump int. ( $\text{J}/\text{m}^2 \text{ s}$ )	Overall gain	Remarks
Ruby	Air	200	$\approx 10$	$3.6 \times 10^{10}$		Dark burns
Ruby	Glycerol	100	$\approx 40$	$3.6 \times 10^{11}$	1.02–1.04	
Ruby	Glycerol	100	$\approx 40$	$7.3 \times 10^{11}$		Gas bubbles
Ti:sapphire	Air	100	$\approx 10$	$1.6 \times 10^{11}$	1.16–1.18	
Ti:sapphire	Air	100	$\approx 10$	$2.5 \times 10^{11}$	1.25–1.31	
Ti:sapphire	Air	100	$\approx 10$	$3.6 \times 10^{11}$	$\approx 1.30$	
Ti:sapphire	Air	175	$\approx 10$	$2.1 \times 10^{11}$	$\approx 1.38$	
Ti:sapphire	Air	175	$\approx 10$	$3.0 \times 10^{11}$	$\approx 1.42$	
Ti:sapphire	Air	100	$\approx 10$	$6.0 \times 10^{11}$		Struc. change
Backscattering data						
Material	in	$L$ ( $\mu\text{m}$ )	$l$ ( $\mu\text{m}$ )	Pump int. ( $\text{J}/\text{m}^2 \text{ s}$ )	Overall gain	$l_g$ (mm)
Ti:sapphire	Water	1000	40	$6.0 \times 10^{11}$	1.36	13.9
Ti:sapphire	Water	1000	40	$6.9 \times 10^{11}$	1.71	11.2
Ti:sapphire	Water	1000	28	$6.5 \times 10^{11}$	2.15	13.4
Ti:sapphire	Air <sup>a</sup>	1000	18	$6.5 \times 10^{11}$	2.34	18.6
Ti:sapphire	Air <sup>a</sup>	1000	18	$6.9 \times 10^{11}$	2.55	18.5

<sup>a</sup>The medium consists of wet Ti:sapphire particles surrounded by air, and  $l$  is therefore somewhat larger than for a completely dry Ti:sapphire powder.

sample was about 200 mJ (pulse duration 14 ns), which for a beam diameter of 5 mm corresponds to a maximum incident intensity of  $7.3 \times 10^{11} \text{ J}/\text{m}^2 \text{ s}$ . A low intensity probe pulse was incident at a time delay of 14 ns after the pump pulse, on the same side of the sample. (Probe pulse energy 40  $\mu\text{J}$ , pulse duration 14 ns, and beam diameter 5 mm. Probe and pump beam overlap spatially on the sample surface.) The temporal profile of the transmitted and backscattered intensity was recorded. The overall amplification in transmission and in backscattering was determined by comparing the probe intensity with and without pump light. To avoid artifacts from long term effects (like cumulative heating of the sample), the repetition rate of the probe was chosen twice as high at the pump repetition rate, so every second probe shot could serve as a reference measurement without pump light.

In Table II, the results are listed for various ruby and Ti:sapphire samples. The samples have a slab geometry with thickness 1 mm. We found that for dry powdered ruby sample, single shot heating poses a problem. Already at modest pump intensities ( $3.6 \times 10^{10} \text{ J}/\text{m}^2 \text{ s}$  corresponding to 10 mJ in 14 ns on an area of  $20 \text{ mm}^2$ ), dark burns occur on the sample surface after a few pump pulses. By suspending the ruby powder in glycerol, this problem is partly solved, however, in that case at high intensities, gas bubbles occur in the sample. The overall gain that is observed with ruby is very small (1.02–1.04), and because ruby is a three level system with a large absorption at the laser wavelength, the

observed overall gain is merely reduced absorption. For powdered Ti:sapphire, the problems with heating are much smaller. Only for the dry Ti:sapphire powders at high intensities ( $6.0 \times 10^{11} \text{ J}/\text{m}^2 \text{ s}$  corresponding to 165 mJ in 14 ns on an area of  $20 \text{ mm}^2$ ), we see a small structural change of the sample surface after a few hours. The obtained overall gain for Ti:sapphire samples is high both in reflection ( $> 2.0$ ) and in transmission ( $\approx 1.4$ ).

Also listed for the backscattering data in Table II is the average gain length in the sample, which was calculated from the overall gain using diffusion theory (see Refs. [6,15]). The theoretical shortest gain length (100% excitation) for these samples is 2.3 mm.

The above results show that it is possible to realize an amplifying random medium on which scattering experiments can be performed. Using powdered Ti:sapphire, average gain lengths on the order of 10 mm can be obtained in a large (several  $\text{mm}^3$ ) and reasonably strongly scattering ( $l \lesssim 20 \mu\text{m}$ ) medium. Experiments have to be performed, however, with pulsed light at a low repetition rate. We have used the powdered Ti:sapphire samples to perform coherent backscattering experiments, which are described in Ref. [6].

#### IV. RANDOM LASERS

The output of an amplifying random medium can show characteristics that are very similar to laser action. As we

saw in Sec. II, the amplified spontaneous emission from such a system can be pulsed. Also, due to gain narrowing, the amplified spontaneous emission can be spectrally narrow. It is tentative to call this system a random laser, however, one has to be careful.

Laser action requires the presence of some sort of optical cavity. When the loss rate of this cavity becomes smaller than the spontaneous emission rate, laser action can take place in the specific *modes* corresponding to this cavity. In that case the number of photons in a specific mode will become (much) larger than one and the output will be spectrally narrow and coherent. Concerning amplifying random media, one can distinguish three regimes, depending on the amount of scattering.

#### A. Weak scattering and gain

If the scattering is very weak, that is,  $l$  is of the order of the sample size, the role of the scatterers is trivial. If we pump a clear laser material in a certain geometry, amplified spontaneous emission will build up in the direction of largest gain, which is generally the direction in which the excited region is most extended. This yields a directionality in the output of the system. Due to gain narrowing, the spectrum of ASE can be very narrow as in the output of a laser. Also, the pulse length of the ASE output can be much shorter than the lifetime of the excited state of the laser material. If one adds some scatterers to the clear laser material, the directionality of the ASE is scrambled, and in all directions the output will be spectrally narrow and will decay rapidly. In this regime of weak scattering, the only role of the particles is to scramble the directionality of the ASE, which would build up also in the absence of scatterers. This was the effect observed in Ref. [7], where very weakly scattering dye solutions (with  $l \approx$  sample size) were studied.

#### B. Modest scattering and gain

If the scattering is stronger, that is  $l$  is much smaller than the sample size but still larger than the wavelength, the presence of scatterers influences the spectral and temporal properties of the output. Due to the scattering, the residence time of the light in the sample is largely increased compared to a clear sample without scatterers. A gain narrowing process will therefore be much more efficient, and the presence of scatterers can therefore narrow the spectrum of the output.

As we saw in Sec. II, modest scattering with gain can also lead to a pulsed output. As mentioned before, this pulsed output was also observed in Ref. [8], where the emission characteristics from powdered laser crystals were studied.

#### C. Strong scattering and gain

If we even further increase the scattering strength we reach the situation where  $l$  becomes equal to or smaller than the wavelength. This is the regime where Anderson localization of light is expected to occur [1]. Due to very strong scattering, recurrent scattering events arise [18]. These are scattering events in which the light returns to a scatterer from which it was scattered before, thereby forming closed loop paths. If the amplification along such a loop path would be strong enough, they could serve as random ring cavities for the light. In that case the system would lase in the modes allowed by these random ring cavities.

A strongly scattering medium with gain could open interesting possibilities in the search for Anderson localization of light [19]. So far, no experimental evidence for Anderson localization of light waves has been found because it is difficult to obtain samples that scatter sufficiently. The transition to a localized state could be assisted by the introduction of gain: the occurrence of ‘‘random ring cavities’’ could increase the importance of recurrent events, thereby lowering the amount of scattering required to obtain localization.

From an experimental point of view, it is, however, not trivial to obtain strong scattering and amplification. One option would be to dope TiO<sub>2</sub> particles with, e.g., a Rhodamine laser dye. The disadvantage of such a system is that the lifetime of the excited state is very short, and experiments with a probe pulse will have to be performed with picosecond time resolution. Another option would be to use mixtures of a strongly scattering material such as TiO<sub>2</sub> powder with powdered Ti:sapphire.

#### ACKNOWLEDGMENTS

We wish to thank Meint van Albada for discussions. The work in this paper is part of the research program of the ‘‘Stichting voor Fundamenteel Onderzoek der Materie’’ (Foundation for Fundamental Research on Matter) and was made possible by financial support from the ‘‘Nederlandse Organisatie voor Wetenschappelijk Onderzoek’’ (Netherlands Organization for the Advancement of Research).

- 
- [1] For recent reviews, see *Classical Wave Localization*, edited by P. Sheng (World Scientific, Singapore, 1990); *Analogies in Optics and Micro Electronics*, edited by W. van Haeringen and D. Lenstra (Kluwer, Dordrecht, 1990); P. Sheng, *Introduction to Wave Scattering, Localization, and Mesoscopic Phenomena* (Academic, San Diego, 1995).
- [2] Y. Kuga and A. Ishimaru, *J. Opt. Soc. Am. A* **8**, 831 (1984); M.P. van Albada and A. Lagendijk, *Phys. Rev. Lett.* **55**, 2692 (1985); P.E. Wolf and G. Maret, *ibid.* **55**, 2696 (1985).
- [3] S. Feng, C. Kane, P.A. Lee, and A.D. Stone, *Phys. Rev. Lett.* **61**, 834 (1988); J.F. de Boer, M.P. van Albada, and A. Lagendijk, *Phys. Rev. B* **45**, 658 (1992).
- [4] V.S. Letokhov, *Zh. Éksp. Teor. Fiz.* **53**, 1442 (1967) [*Sov. Phys. JETP* **26**, 835 (1968)].
- [5] B. Davison and J.B. Sykes, *Neutron Transport Theory* (Oxford University Press, Oxford, 1958).
- [6] D.S. Wiersma, M.P. van Albada, and A. Lagendijk, *Phys. Rev. Lett.* **75**, 1739 (1995).
- [7] N.M. Lawandy, R.M. Balachandran, A.S.L. Gomes, and E. Sauvain, *Nature* **368**, 436 (1994).
- [8] C. Gouedard, D. Husson, C. Sauteret, F. Auzel, and A. Migus, *J. Opt. Soc. Am. B* **10**, 2358 (1993).
- [9] Note that direct absorption and stimulated emission of pump, respectively, probe without scattering is not taken into account.

This is justified due to the fact that in our case the scattering is always much stronger than the absorption and stimulated emission. Taking direct absorption and stimulated emission into account requires adding (two) appropriate terms to Eq. (6), and allowing the extinction coefficient in Eqs. (8) and (9) to become place and time dependent.

- [10] H.C. van de Hulst and R. Stark, *Astron. Astrophys.* **235**, 511 (1990).
- [11] W.H. Press, B.P. Flannery, S.A. Teukolsky, and W.T. Vetterling, *Numerical Recipes* (Cambridge University Press, New York, 1989).
- [12] In fact, the system becomes unstable if  $L_{cr} \leq L + 2z_0$ . In other words, for the stability criterion the relevant system size is the physical thickness plus the extrapolation length.
- [13] At large sample thicknesses, the spatial profile of the pump energy density starts to play a role, which makes the relation between the obtained excitation level and the sample thickness more complex.
- [14] See, for instance, A.E. Siegman, *Lasers* (Oxford University Press, New York, 1986).
- [15] D.S. Wiersma, Ph.D. thesis, University of Amsterdam, 1995.
- [16] The higher internal energy density in the scatterers compared to their environment [17] is not taken into account. This would yield somewhat smaller values of  $l_i$ , which would result in more efficient pumping.
- [17] A. Bott and W. Zdunkowski, *J. Opt. Soc. Am. A* **4**, 1361 (1987).
- [18] D.S. Wiersma, M.P. van Albada, B.A. van Tiggelen, and A. Lagendijk, *Phys. Rev. Lett.* **74**, 4193 (1995).
- [19] P. Pradhan and N. Kumar, *Phys. Rev. B* **50**, 9644 (1994); Z. Zhang, *ibid.* **52**, 7960 (1995).